JOURNAL OF GENERAL VIROLOGY

RESEARCH ARTICLE

Mutso *et al.*, *Journal of General Virology* 2017;98:2712–2724

DOI 10.1099/jgv.0.000938

Reverse genetic system, genetically stable reporter viruses and packaged subgenomic replicon based on a Brazilian Zika virus isolate

Margit Mutso,[1,2]† Sirle Saul,[1]† Kai Rausalu,[1] Olga Susova,[3] Eva Žusinaite,[1] Suresh Mahalingam[2] and Andres Merits[1,*]

Abstract

Zika virus (ZIKV, genus *Flavivirus*) has emerged as a major mosquito-transmitted human pathogen, with recent outbreaks associated with an increased incidence of neurological complications, particularly microcephaly and the Guillain–Barré syndrome. Because the virus has only very recently emerged as an important pathogen, research is being hampered by a lack of reliable molecular tools. Here we report an infectious cDNA (icDNA) clone for ZIKV isolate BeH819015 from Brazil, which was selected as representative of South American ZIKV isolated at early stages of the outbreak. icDNA clones were assembled from synthetic DNA fragments corresponding to the consensus sequence of the BeH819015 isolate. Virus rescued from the icDNA clone had properties identical to a natural ZIKV isolate from South America. Variants of the clone-derived virus, expressing nanoluciferase, enhanced green fluorescent or mCherry marker proteins in both mammalian and insect cells and being genetically stable for multiple *in vitro* passages, were obtained. A ZIKV subgenomic replicon, lacking a prM- and E glycoprotein encoding region and expressing a *Gaussia* luciferase marker, was constructed and shown to replicate both in mammalian and insect cells. In the presence of the Semliki Forest virus replicon, expressing ZIKV structural proteins, the ZIKV replicon was packaged into virus-replicon particles. Efficient reverse genetic systems, genetically stable marker viruses and packaged replicons offer significant improvements for biological studies of ZIKV infection and disease, as well as for the development of antiviral approaches.

INTRODUCTION

Zika virus (ZIKV) is a member of the *Flavivirus* genus. It was first isolated in 1947 from a rhesus monkey in Uganda, with the first human infection recorded in 1954. For the next 50 years, human infections were reported very rarely. More recently, ZIKV has emerged as a major mosquito-transmitted human pathogen [1, 2]: from 2007 onwards there have been numerous ZIKV outbreaks in the Pacific region, starting in Micronesia and with a particularly intense outbreak in French Polynesia in 2013 with about 30 000 symptomatic cases [3, 4]. In 2015, ZIKV emerged in the Americas and rapidly spread throughout the region [5, 6]. The majority of ZIKV infections are asymptomatic, while symptomatic cases are usually benign, with mild features including fever and rash.

ZIKV has two different lineages: African and Asian [7]. The recent ZIKV outbreaks have been caused by viruses belonging to the Asian lineage and have been associated with an increased incidence of neurological complications, particularly microcephaly and the Guillain–Barré syndrome [8–10]. The evidence that ZIKV is a cause of these neurological complications is now strong [11, 12], and it is these complications that make the emergence of ZIKV an international health emergency. Due to its very recent emergence, there is a severe paucity of experimental tools for basic research and development of antiviral strategies. In particular, there is an urgent need for infectious cDNA (icDNA) clone-derived viruses based on clinical (patient-derived) parental viruses that can be engineered into viruses expressing marker genes for use in cell culture experiments and in animal models.

Received 30 May 2017; Accepted 18 September 2017

Author affiliations: [1]Institute of Technology, University of Tartu, Tartu, Estonia; [2]Institute for Glycomics, Griffith University, Gold Coast Campus, Southport, 4222, Queensland, Australia; [3]Blokhin Russian Cancer Research Center, Ministry of Health of the Russian Federation, Moscow, 115487, Russia.

***Correspondence:** Andres Merits, andres.merits@ut.ee

Keywords: Zika virus; flavivirus; reverse genetics; infectious cDNA; reporter protein; replicon.

Abbreviations: CPE, cytopathic effect; DMEM, Dulbecco's modified Eagle's medium; EGFP, enhanced green fluorescent protein; FfLuc2, firefly luciferase 2; FMDV, foot-and-mouth disease virus; Gluc, *Gaussia* luciferase; HCMV, human cytomegalovirus; HDV, hepatitis delta virus; icDNA, infectious cDNA; IRES, internal ribosome entry site; NanoLuc, nanoluciferase; RLU, relative luciferase units; RSLuc, red-shift luciferase from *Luciola italica*; SFV, Semliki Forest virus; SV40, simian virus 40; VREP, virus replicon particle; ZIKV, Zika virus.

†These authors contributed equally to this work.

Three supplementary figures are available with the online Supplementary Material.

Shan and colleagues recently described the generation of the first icDNA clones based on Asian lineage ZIKV, using an isolate obtained prior to the South American outbreak. This study highlighted the utility of icDNA clone-derived ZIKV for anti-viral screening, in an immunodeficient mouse model [13], and for studies of evolutionary enhancement of ZIKV infectivity in *Aedes aegypti* mosquitoes [14]. Subsequently, an icDNA clone of ZIKV from African lineage virus was constructed [15], as well as several clones representing different isolates originating from America [16–20]. Despite these successes, there is a need for further tools including icDNA clones of clinically relevant South American ZIKV isolates suitable for construction and rescue of genetically stable recombinant viruses expressing a wider range of reporters such as fluorescent proteins or luciferases.

This report describes the generation of molecular tools for ZIKV research including icDNA-derived viruses stably expressing nanoluciferase (NanoLuc), enhanced green fluorescent protein (EGFP) and mCherry reporters and a replicon vector with a packaging system. These clones were based on the sequence of one of the earliest Brazilian ZIKV isolates, BeH819015, a representative of the most prominent group of South American ZIKV isolates. Unlike a previously constructed reverse genetics system involving four high-copy plasmids based on the same isolate [20], our system is based on a single low-copy plasmid. It is not only fully synthetic but its sequence corresponds almost exactly to that of the published consensus sequence of the isolate, including also synonymous differences from other South American isolates. Our data reveals that biological *in vitro* properties of clone-derived ZIKV are identical to those of closely related natural ZIKV isolated from South America.

RESULTS

Design and construction of ZIKV icDNA clones

To select a representative isolate, genome and polyprotein sequences from ZIKV isolated at early stages of the South American outbreak were aligned. The polyprotein of ZIKV isolate BeH819015 (GI : 975885966), a representative of the most prominent group of ZIKV isolates from South America [20], was found to be closest to the existing consensus sequence. Importantly, BeH819015-encoded polyprotein contained no sequence deviation that could be attributed to random variation, specific adaptations and/or sequencing errors. The missing nucleotides of the 5′-UTR and 3′- UTR (first 13 and last 67 nucleotides of genome, respectively) were taken from ZIKV isolate PE243/2015 from Brazil (GI : 1026288139). Subsequent analysis carried out using all (20 in total by mid-July 2017) completely sequenced genomes of ZIKV isolates from South and North America available in the database revealed that the used 3′ sequence is identical in all isolates and that the 5′ sequence is also highly conserved. Thus, it is very likely that the sequences from PE243/2015 are identical to those of BeH819015.

The ZIKV icDNA clone was designed based on a next-generation-derived sequence (GI : 975885966) and constructed from synthetic DNAs. Three versions of the icDNA clone were made: two relied on *in vitro* transcription from an SP6 promoter, while the third design contained a cytomegalovirus (CMV) early promoter, a simian virus 40 (SV40) late termination sequence and an intron interrupting the ZIKV polyprotein reading frame. Each of the constructs was assembled from four synthetic DNA fragments (Fig. 1a); from these, fragment B was impossible to clone into a high-copy number plasmid. Similarly, attempts to assemble the full-length icDNA clones in high-copy number plasmids were unsuccessful, regardless of the presence of introns in the capsid and/or NS1 protein encoding regions of ZIKV cDNA. The largest cDNA construct in the high-copy number plasmid was pUC-SP6-ZIKV-Del (Fig. S1, available in the online Supplementary Material), harbouring a deletion corresponding to residues 1538–3344 of the ZIKV genome. The fragment corresponding to the missing part was, however, stable when inserted into the high-copy number plasmid, thus allowing construction of a two-plasmid ZIKV icDNA system (Fig. S1). This system was successfully used to rescue wt and marker protein-expressing viruses (Figs S2 and S3), although the rescue was relatively slow: the cytopathic effect (CPE) was detected at day 9–10 post transfection (p.t.). To overcome this issue we assembled three single-plasmid icDNA clones designated as pCCI-SP6-ZIKV, pCCI-SP6-ZIKV-Rz and pCCI-CMV-ZIKV using a single-copy plasmid as the backbone. All of these plasmids were stable when propagated in bacteria.

Rescue and properties of icDNA-derived wt ZIKV BeH819015

When Vero cells were transfected with transcripts from pCCI-SP6-ZIKV, pCCI-SP6-ZIKV-Rz or with pCCI-CMV-ZIKV plasmid, CPE was detected by day 5–8 p.t. Successful rescue of ZIKV from pCCI-CMV-ZIKV and pCCI-SP6-ZIKV-Rz was confirmed by Western blot (Fig. 1b). The p0 virus stocks rescued from pCCI-CMV-ZIKV, pCCI-SP6-ZIKV and pCCI-SP6-ZIKV-Rz had titres 4.3×10^4, 1.1×10^6 and 6.2×10^5 p.f.u. ml^{-1}, respectively, and all three rescued viruses produced a similar set of plaques of variable size (Fig. 1c). As viruses with RNA genomes are prone to rapid cell-culture adaptation, we tested the effect of passage up to four times on virus rescued from pCCI-SP6-ZIKV. Stocks from the later passages caused CPE at earlier time points, indicating possible adaptation to growth in cell culture. Therefore, RNA from the p4 virus was isolated and the coding region sequenced. A single-point mutation was identified, C3895T, which resulted in a change of amino acid residue in NS2A protein (Ala 117 to Val; corresponds to Ala1263 Val in ZIKV polyprotein). This mutation could also be detected in early (p1) passage stock from this rescue experiment but not in stocks originating from independent rescues. The role of this mutation in cell-culture adaptation of ZIKV and its possible contribution to the heterogeneous plaque morphology of rescued viruses (Fig. 1c) remains

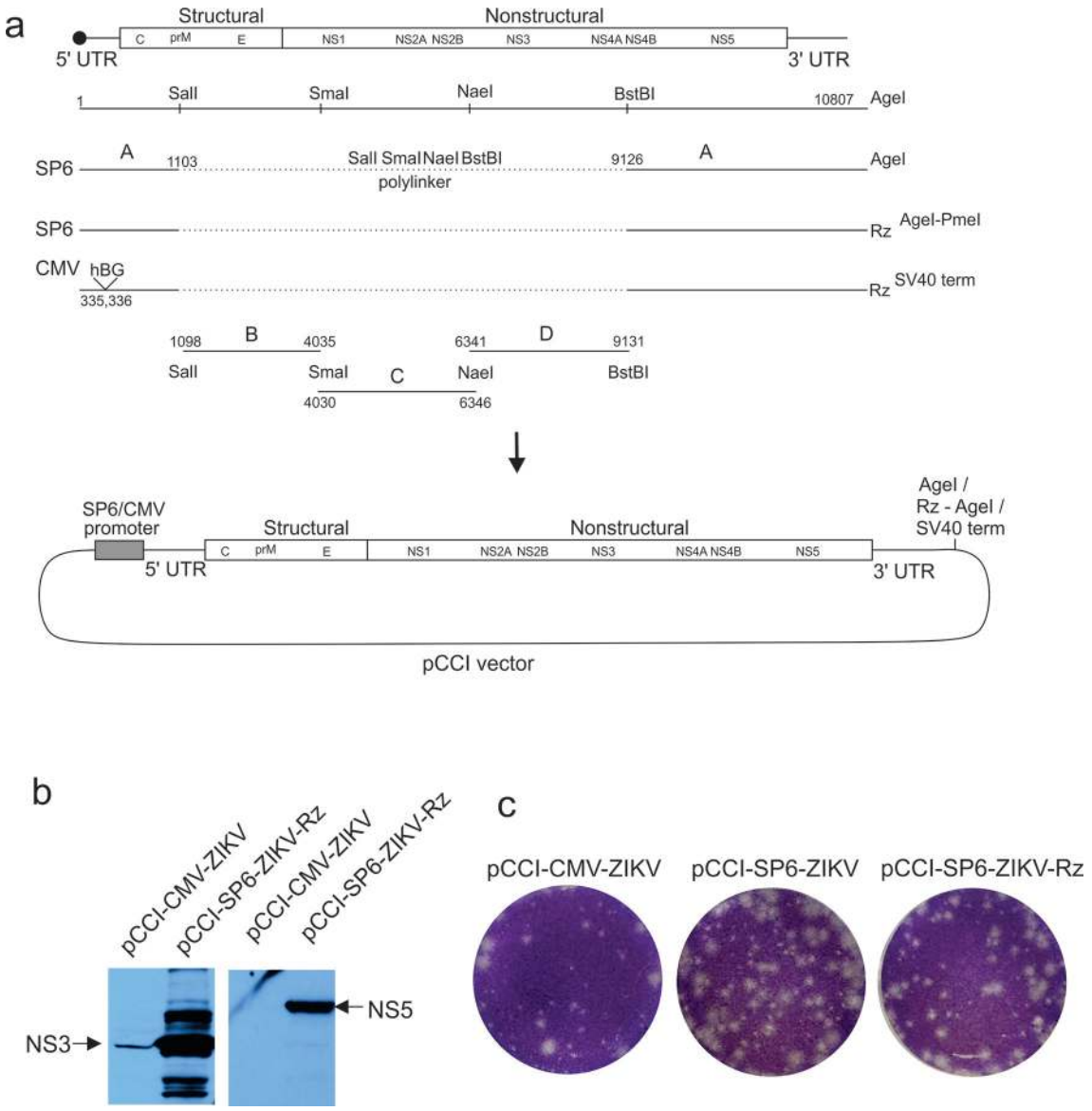

Fig. 1. Construction of ZIKV icDNA clones and rescue of wt ZIKV. (a) Schematic representation of the strategy used for constructing the icDNA clone of ZIKV and the assembly process of CMV-, SP6- and SP6-Rz designs in a CopyControl pCC1BAC vector. Genome organization, unique restriction sites used for cloning, and their positions in the ZIKV genome are shown. SP6 – promoter for SP6 RNA polymerase; Rz – antigenomic strand ribozyme of HDV; CMV – HCMV early promoter. The positions of the second intron from human beta globin gene (hBG), removed by splicing, and the SV40 late polyadenylation region (SV40 term) are shown. (b) Western blot analysis of ZIKV proteins in lysates of Vero cells electroporated with pCCI-CMV-ZIKV or *in vitro* transcripts of pCCI-SP6-ZIKV-Rz (right panel). Cells were collected upon development of CPE; lysate corresponding to 50 000 transfected cells was loaded into each lane; antibodies against ZIKV NS3 and ZIKV NS5 were used to detect corresponding proteins. The band corresponding to NS5 protein for virus rescued from pCCI-CMV-ZIKV, poorly visible on used exposure, was clearly detected when filters were over-exposed. (c) Plaque morphology of pCCI-CMV-ZIKV-, pCCI-SP6-ZIKV- and pCCI-SP6-ZIKV-Rz-derived viruses. Vero cells were infected at low m.o.i., and plaques were stained at 4 days p.i.

unknown. However, if this does represent an adaptive mutation, it is just one of several potential adaptive mutations as growth acceleration during passaging was also observed for ZIKV-EGFP, ZIKV-NanoLuc and ZIKV-mCherry even though p4 stocks of these viruses did not contain the C3895T mutation.

Next we determined how closely the properties of the virus, rescued from icDNA clone icBeH819015 (to exclude the possible impact of C3895T mutation a p1 stock obtained from an independent rescue experiment using pCCI-SP6-ZIKV was used), corresponded to parental virus. As we did not have access to the original ZIKV BeH819015 isolate, the

ZIKV PRVABC59 strain was used instead. These two strains are closely related, with only 24 nucleotide differences between them (sequence identity 99.78 %): three differences map to the 3′-UTR and 21 to the coding region. Only three changes in the coding region are non-synonymous and result in a change in amino acid residue (T80I, L620V and V2601A). Thus, the identity of sequences of encoded polyproteins is 99.91 %. Multi-step (m.o.i. 0.1) growth curves were obtained from Vero and two human cell lines relevant for ZIKV infection: neuronal (D3) and placental (BeWo) cells. Both viruses showed highly similar growth kinetics in all three cell types (Fig. 2). Finally, we compared localization of ZIKV envelope protein, NS3 protein, NS5 protein and dsRNAs (marker of viral replicase complexes) in infected Vero cells. Again, no significant differences were observed between icBeh819015 and PRVABC59. In both cases, envelope protein and NS3 localized in the cytoplasm of the infected cells and co-localized with viral dsRNAs, while NS5 mostly localized in nuclei (Fig. 3). Taken together, these data confirm the *in vitro* phenotype of virus rescued from synthetic icDNA is identical to that of related patient-derived ZIKV isolated from South America. Thus, we concluded that the synthetic consensus sequence-based icDNA clones do not contain any accidental (sequencing) errors or specific adaptations that would affect virus rescue or result in rescued viruses with properties different from those of parental virus, as has been previously reported by others [16, 20].

Construction and rescue of ZIKV variants with inserted markers

The marker insertion strategy, allowing expression in both insect and mammalian cells, was adopted from strategies previously used for different Flaviviruses [21, 22] (Fig. 4a). In all cases, sequences encoding for markers were inserted between two copies of the capsid protein gene and, in order to reduce potential recombination between the duplicated sequences, the codon usage of the downstream copy was altered. Altogether eight different variants of icDNA were constructed. Three of them (with NanoLuc, EGFP and mCherry markers) also contained a ubiquitin sequence between foot-and-mouth disease virus (FMDV) 2A autoprotease and the duplicated copy of capsid protein (Fig. 4a).

Infectious viruses were successfully rescued using the two-plasmid vector strategy with pUC-SP6-ZIKV-Del-EGFP or pUC-SP6-ZIKV-Del-NanoLuc and pKS-BShort. CPE was observed at 9 days p.t., and expression of NS3, NS5 and EGFP (for ZIKV-EGFP) was confirmed by Western blotting (Fig. S3). Rescue of reporter viruses using single-plasmid vectors (pCCI-SP6-ZIKV-EGFP and others) was, again, significantly faster: for ZIKV expressing EGFP, NanoLuc or mCherry markers, CPE became evident on day 6 p.t. In contrast, only limited CPE was observed for viruses expressing firefly luciferase 2 (FfLuc2) and red-shift luciferase from *Luciola italica* (RSLuc) at day 8 p.t. With the exception of ZIKV-FfLuc2 (titres 4.5×10^3), the p0 stocks of recombinant viruses had titres 5.7×10^5–2.4×10^6 p.f.u. ml^{-1}, which is similar to wt icBeH819015 virus. In this experiment no clear differences between ZIKV-EGFP and ZIKV-EGFP-Ubi or ZIKV-mCherry and ZIKV-mCherry-Ubi were observed. NanoLuc activities in Vero cells infected by ZIKV-NanoLuc and ZIKV-NanoLuc-Ubi were high and similar to each other (>2×10^7 RLU per 10 000 cells). These data indicate that insertion of ubiquitin offered no benefit for ZIKV rescue, replication and marker protein expression.

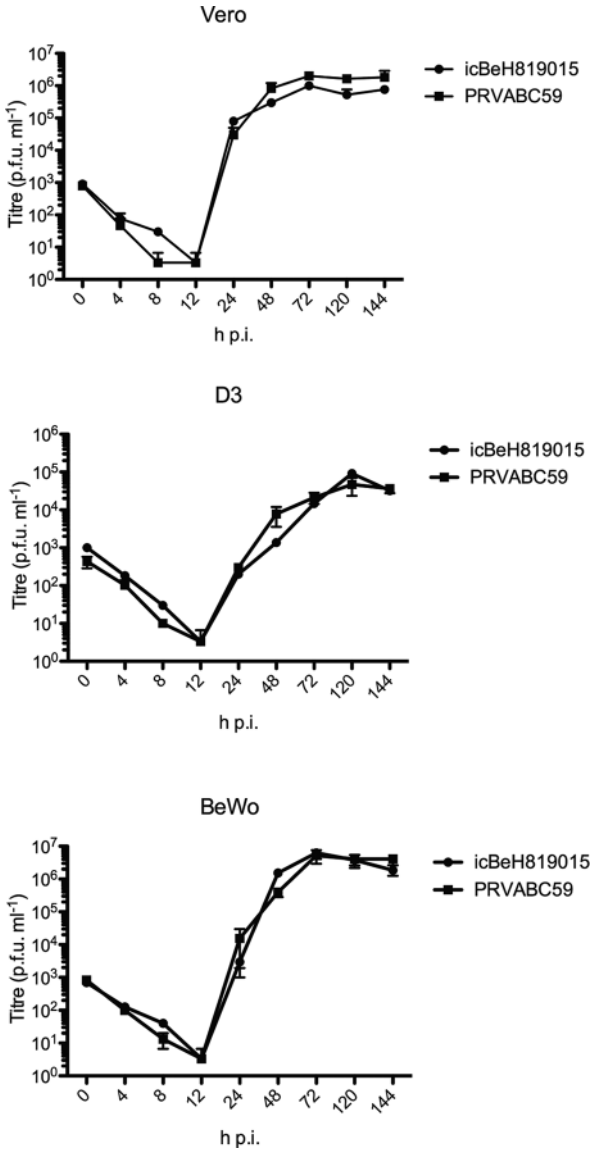

Fig. 2. Multi-step growth curves of ZIKV PRVABC59 strain and icDNA-derived icBeH819015 virus. Vero, D3 and BeWo cells were infected with PRVABC59 and with p1 stock of icBeH819015 at m.o.i. of 0.1. The culture medium was collected at indicated time points, and the amount of released infectious virions was analysed by plaque titration. Results of one experiment performed in triplicate are presented; the experiment was repeated twice with similar results.

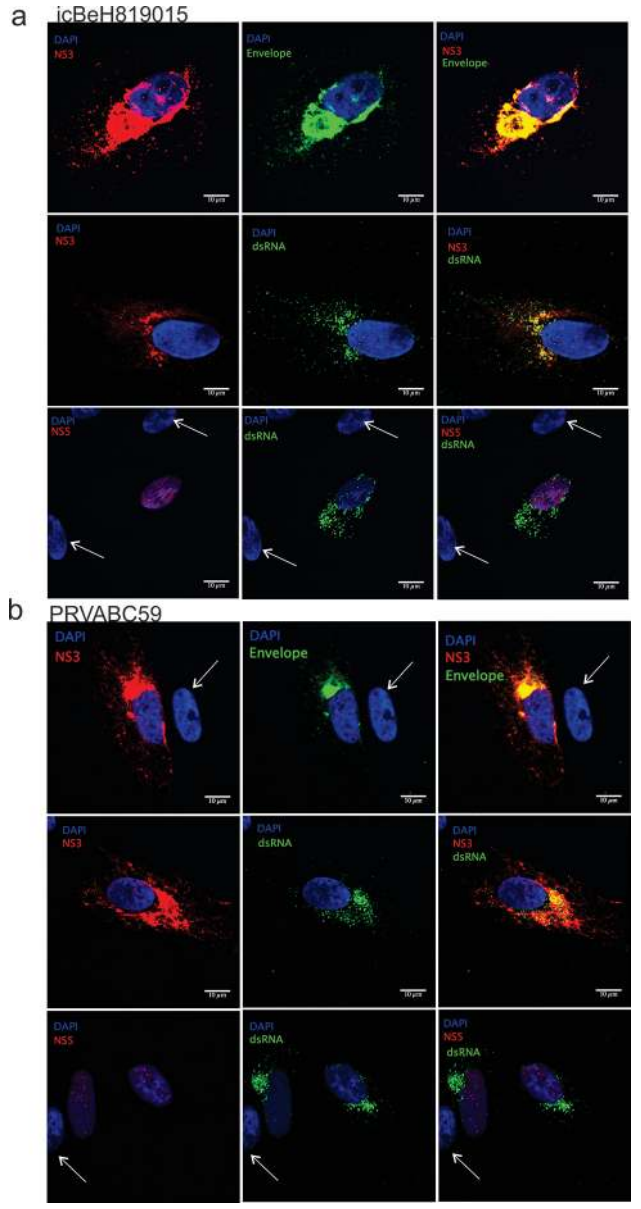

Fig. 3. Localization of ZIKV dsRNA, envelope, NS3 and NS5 proteins in Vero cells infected with PRVABC59 and icBeH819015. Vero cells grown on coverslips were infected with icBeH819015 (a) or PRVABC59 (b) at m.o.i. of 1. Non-infected cells (pointed out by arrows) served as negative controls. At 24 h p.i., the cells were fixed and stained with different combinations of rabbit anti-NS3 antisera (red), rabbit anti-NS5 antisera (red), mouse pan-flavivirus anti-envelope antibody (green) and mouse monoclonal antibody against dsRNA (green). Nuclei were counterstained with DAPI (blue). Co-localization of red and green signals is shown as yellow.

Genetic stability of ZIKV harbouring markers in cell culture

The stability of FfLuc2, RSLuc and NanoLuc expression by recombinant ZIKV was first estimated by measuring reporter activity in transfected Vero cells and in cells infected with p0–p4 stocks of the corresponding viruses. In transfected cells, all four viruses expressed marker protein at high levels (luciferase reads $>10^7$ RLU per 10 000 cells). NanoLuc expression levels remained stably high throughout all passaging experiments for both ZIKV-NanoLuc and ZIKV-NanoLuc-Ubi (Fig. 4b). In contrast, for viruses harbouring larger FfLuc2 or RSLuc inserts, marker expression rapidly diminished with each passage (Fig. 4b). As virus titres remained high, and the CPE development even accelerated, it is likely that viruses capable of expression of FfLuc or RSLuc were rapidly outcompeted by aberrant viruses. Furthermore, these data suggest that plaques, observed for corresponding stocks, were most likely made by aberrant viruses. Thus, it is possible that viruses with FfLuc2 or RSLuc markers were not only unstable but also unable to form plaques on Vero cells, as has been described for ZIKV expressing a *Renilla* luciferase marker [13].

Second, we analysed the percentage of mCherry positive plaques in Vero cells infected with p0–p4 stocks of ZIKV-mCherry and ZIKV-mCherry-Ubi. Even in the p4 stock, over 90 % of ZIKV-mCherry virions contained genomes capable of expressing marker protein (Fig. 4b). In contrast, the ability of ZIKV-mCherry-Ubi to produce marker-positive plaques decreased in later passages (Fig. 4b); this was accompanied by the appearance of large plaques of somewhat cloudy appearance (Fig. 4c). Similarly, in cells infected with p4 stocks of ZIKV-EGFP-Ubi and ZIKV-EGFP, the EGFP levels expressed by the former were clearly lower (Fig. 4d).

Finally, these observations were confirmed by RT-PCR analysis of genomes isolated from p0, p2 and p4 stocks of NanoLuc, EGFP and mCherry expressing viruses. Again, for EGFP and mCherry marker viruses the genomes lacking ubiquitin insertion were clearly more stable than their counterparts (Fig. 4e). Only NanoLuc, which is the smallest of the inserted markers, was stably maintained in all of the analysed passages regardless of the presence or absence of the ubiquitin insert (Fig. 4e). These data, coupled with the properties of viruses expressing FfLuc2 and RSLuc markers, indicate that the stability of recombinant ZIKV genomes is inversely correlated with the size of the inserted sequences. Thus, while even large luciferases (1600 bp or more) were well expressed in transfected cells (Fig. 4b), only sequences encoding for small (≈700 bp or less) marker protein, in addition to duplicated capsid protein and FMDV 2A insertion, had no adverse effects on ZIKV propagation in cell culture.

In vitro phenotype of ZIKV expressing marker proteins

Next we infected Vero cells with ZIKV-mCherry or ZIKV-EGFP and analysed subcellular localization of virus-encoded proteins. As for wt viruses (Fig. 3), NS3 and envelope protein were detected in the cytoplasm and co-localized with each other. Localization of mCherry and EGFP was also very similar to these viral proteins (Fig. 5). Due to its position in polyprotein of recombinant viruses (immediately

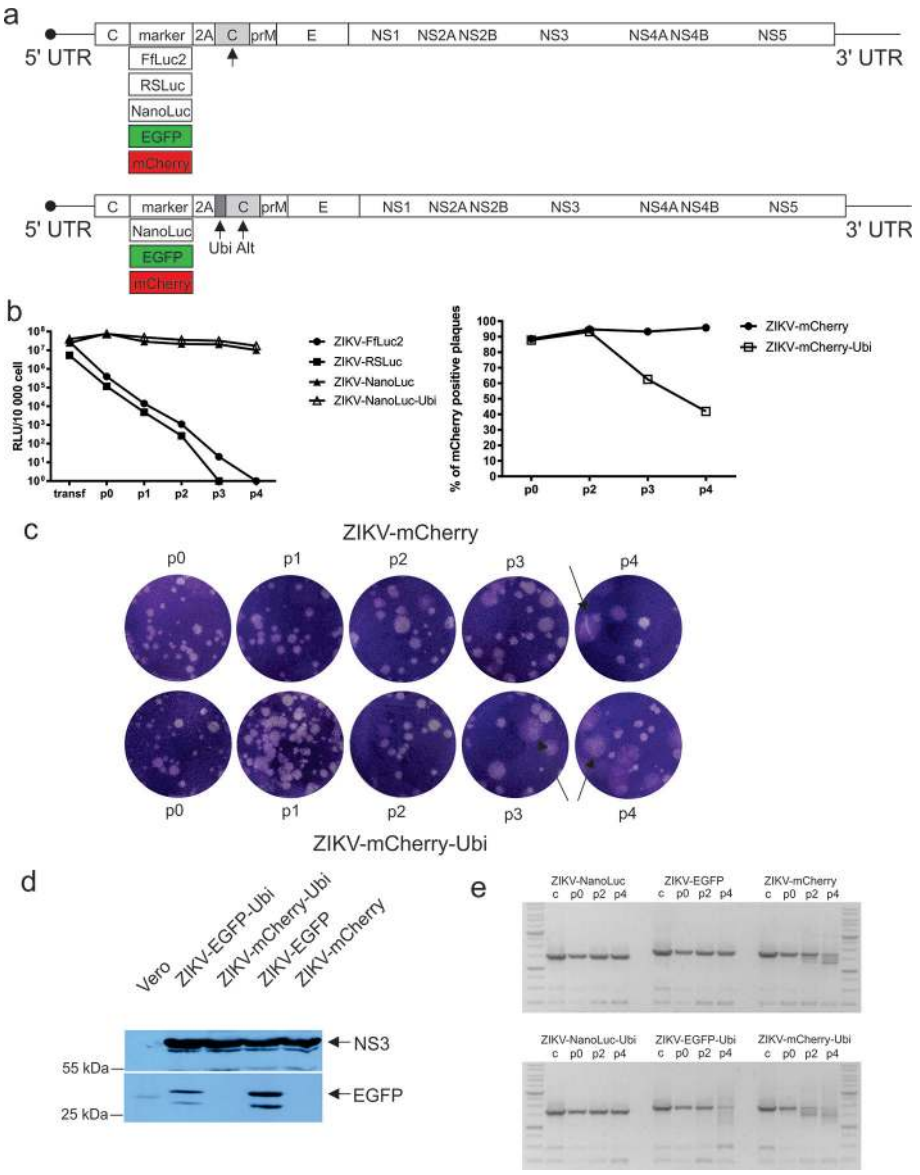

Fig. 4. Strategies used for insertion of markers into ZIKV icDNA and analysis of genetic stability of rescued viruses. (a) Schematic representation of non-Ubi (above) and Ubi (below) designs of recombinant ZIKV icDNAs. Inserted reporters are shown below the drawings; Alt indicates a duplicated copy of the capsid protein-encoding region with altered codons and Ubi indicates sequence encoding for ubiquitin. (b) Stability assays of ZIKV constructs containing reporter genes. Luciferase activity was measured in Vero cells transfected with original transcripts at the time when p0 stock was harvested and for cells infected with p0–p4 virus stocks upon development of CPE. Luciferase activity is presented as relative luciferase units (RLU) per 10 000 cells (left graph). Stability of ZIKV-mCherry and ZIKV-mCherry-Ubi was analysed using a plaque assay on Vero cells. Percentage of mCherry positive plaques from total plaque number was determined for p0–p4 virus stocks (right graph). (c) Morphology of plaques on Vero cells infected with p0–p4 virus stocks of ZIKV-mCherry and ZIKV-mCherry-Ubi. Arrows point to plaques with cloudy appearance. (d) Western blot analysis of proteins from extracts of Vero cells infected at m.o.i. 0.1 with p4 stocks of ZIKV-EGFP-Ubi, ZIKV-mCherry-Ubi, ZIKV-EGFP and ZIKV-mCherry and lysed at 3 days p.i. Lysate corresponding to 50 000 infected cells was loaded on each lane; NS3 and EGFP were detected using corresponding antibodies. (e) Stability analysis of ZIKV-NanoLuc, ZIKV-NanoLuc-Ubi, ZIKV-EGFP, ZIKV-EGFP-Ubi, ZIKV-mCherry and ZIKV-mCherry-Ubi by RT-PCR. RNAs obtained from p0, p2, p4 stocks were reverse transcribed and fragments of cDNA were PCR-amplified using primers corresponding to the 5′-UTR sequence and a primer complementary to the sequence in the beginning of the prM encoding region. PCR fragments obtained using corresponding icDNA clones as templates were used as controls (marked as c).

downstream of C-terminus of capsid protein, Fig. 4a), the marker protein should and did translocate to the lumenal side of endoplasmic reticulum, preventing its diffusion in the cell cytoplasm and/or entry to the nucleus. Thus, all of the analysed proteins, including the markers, had their predicted localization in infected Vero cells.

Finally, C6/36 cells were infected with p3 stocks of ZIKV-NanoLuc and ZIKV-mCherry. As expected, cells infected with ZIKV-mCherry developed intense red fluorescence (not shown). In cells infected with ZIKV-NanoLuc, NanoLuc activity exceeding that measured in mammalian cells ($>2\times10^8$ RLU per 10 000 cells) was observed. These data confirm that the marker insertion strategy did not compromise ZIKV replication or marker expression in vertebrate or mosquito cells.

Properties and packaging system for a ZIKV subgenomic replicon

We constructed ZIKVGlucRep, a subgenomic ZIKV replicon capable of expressing a *Gaussia* luciferase (Gluc) reporter; the replicon contained sequence encoding for mature capsid protein but lacked sequences encoding for preM and, except for the last 30 codons, E proteins (Fig. 6a). Its ability to replicate was analysed in Vero, BHK-21 and C6/36 cells transfected with corresponding *in vitro* transcribed RNAs. Gluc activity in the supernatants of BHK-21 and Vero cells peaked at day 4–5 p.t. and was several-fold higher for BHK-21 cells (Fig. 6b). This indicates that BHK-21 cells are highly permissive for ZIKV RNA replication. Thus, BHK-21 cells can be used for rescue of ZIKV (see Supplementary Material for the corresponding protocol); however, they cannot be used for its propagation as ZIKV BeH819105 was virtually unable to infect them. Thus, our data imply that this defect is due to impaired binding and/or entry of ZIKV into BHK-21 cells. Nevertheless, BHK-21 cells may be suitable for experiments with ZIKV subgenomic replicons. Even higher Gluc activities were measured in supernatants of transfected C6/36 cells indicating that these mosquito cells are particularly permissive for ZIKV RNA replication. Gluc expression in transfected C6/36 cells was short-term and peaked by 48 h p.t. In addition, high intracellular Gluc activity, typically exceeding that in supernatant by two–tenfold, was observed for all cell types, indicating that secretion of Gluc expressed by ZIKVGlucRep was impaired, most likely due to its fusion with the ZIKV capsid and/or FMDV 2A autoprotease (Fig. 6a).

Next we constructed the Semliki Forest virus (SFV)-ZIKV-CprME replicon expressing structural proteins of ZIKV via the subgenomic promoter of SFV (Fig. 6a). Co-transfection of Vero or BHK-21 cells with ZIKVGlucRep and SFV-ZIKV-CprME resulted in a drastic reduction of Gluc expression (compared to cells transfected only with ZIKV-GlucRep). This effect was most likely caused by more rapid replication and high cytotoxicity of the SFV-ZIKV-CprME

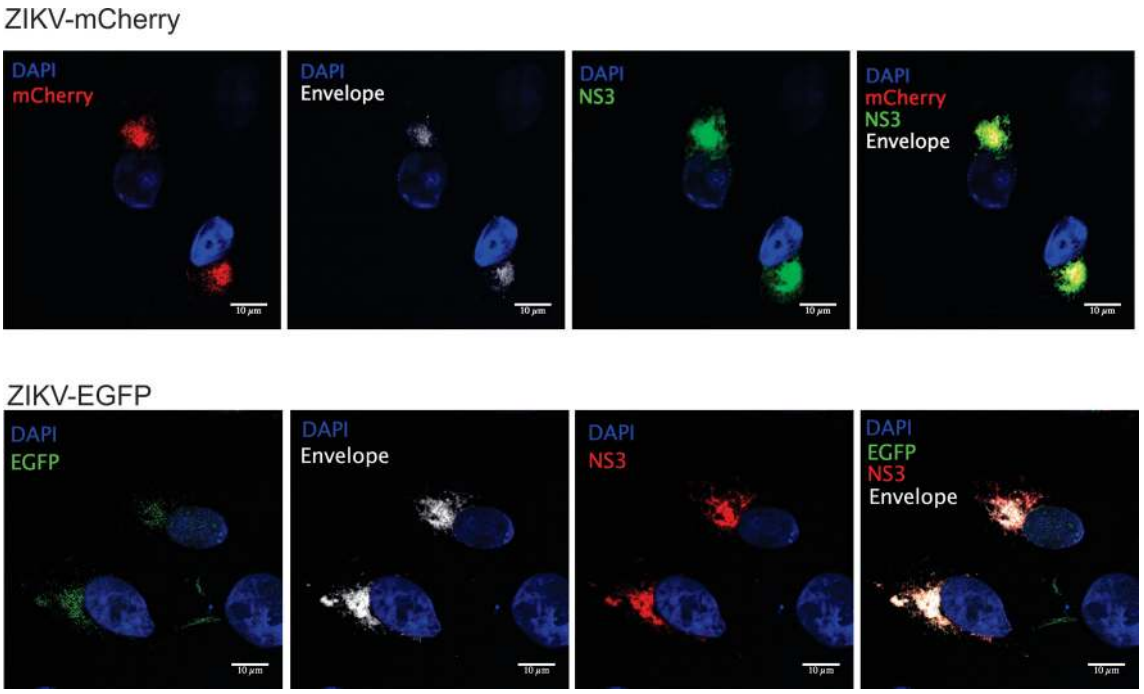

Fig. 5. Localization of fluorescent markers, NS3 and envelope proteins in Vero cells infected with ZIKV-mCherry and ZIKV-EGFP. Vero cells were infected with ZIKV-mCherry and ZIKV-EGFP at m.o.i. of 1. At 24 h p.i. cells were fixed and stained for detection of NS3 localization (shown as green for ZIKV-mCherry-infected cells and as red for ZIKV-EGFP-infected cells) and envelope (white) proteins as described for Fig. 3. mCherry and EGFP were detected by auto-fluorescence; nuclei were counterstained with DAPI.

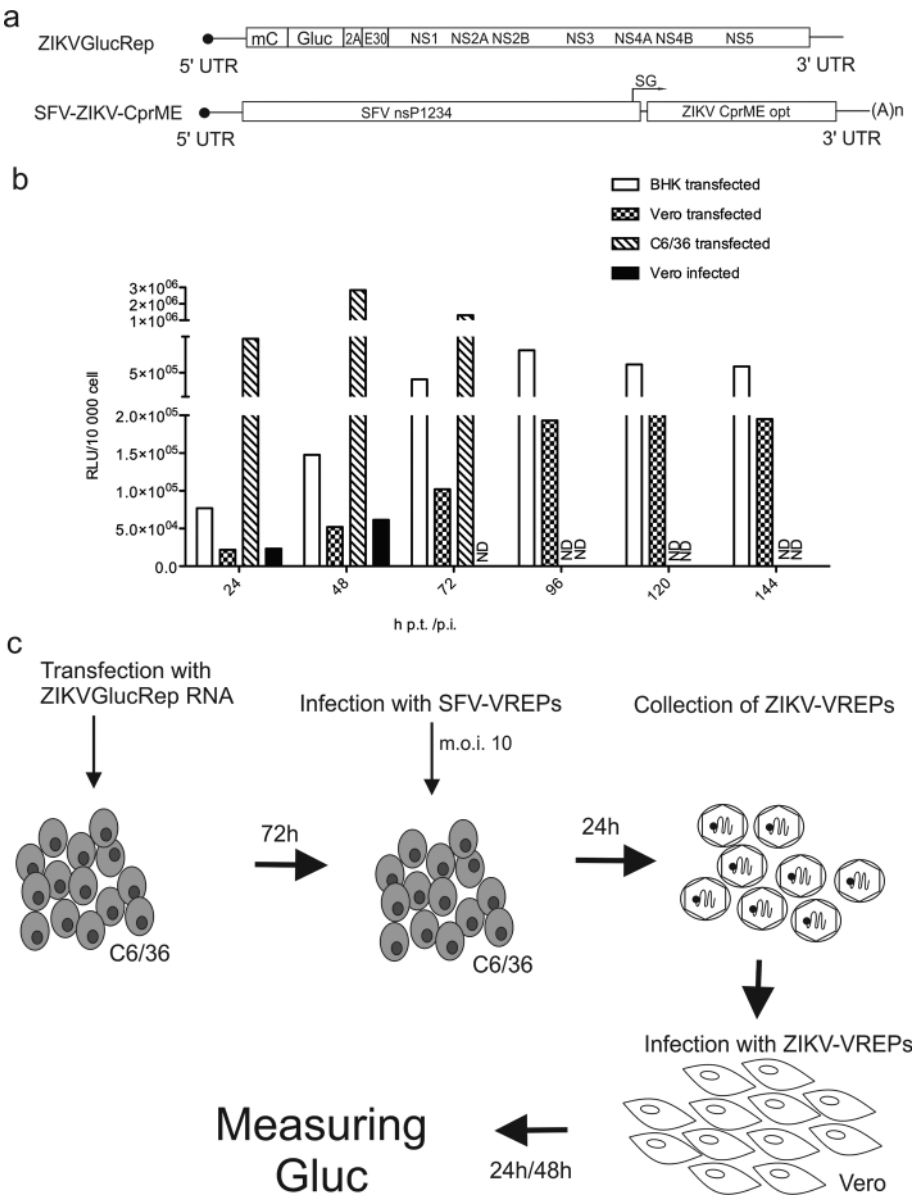

Fig. 6. Construction and packaging of the ZIKV replicon. (a) Schematic representation of the ZIKVGlucRep replicon and the SFV-ZIKV-CprME packaging replicon expressing ZIKV structural proteins from the codon-optimized sequence. mC – mature capsid of ZIKV; E30 – last 30 codons of the ZIKV E-region; SG – SFV subgenomic promoter; CprME opt – codon optimized sequence for expression of structural proteins of ZIKV; (A)n – poly(A) sequence of the SFV replicon. (b) Gluc activity in the supernatants of BHK-21, Vero and C6/36 cells transfected with ZIKVGlucRep replicon RNA and in Vero cells infected with ZIKV-VREPs containing the ZIKVGlucRep replicon. Gluc activity in RLU per 10 000 cell (or supernatant corresponding to 10 000 cells) is shown. Gluc activity in mock-transfected and mock-infected controls (background) was too low to be shown. The experiment was performed twice with similar results. (c) Schematic presentation of the procedure used for production of ZIKV VREPs.

replicon. To overcome this problem, an alternative setup was used for ZIKVGlucRep packaging (Fig. 6c). C6/36 cells were transfected with *in vitro* transcribed ZIKVGlucRep RNA. At 72 h p.t. cells were infected with SFV-virus replicon particles (SFV-VREPs) containing SFV-ZIKV-CprME replicon at m.o.i. 10; 24 h later the supernatant was collected. The presence of the ZIKVGlucRep replicon packaged by ZIKV structural proteins (ZIKV-VREPs) was revealed by a re-infection assay. For this, the supernatant was used to infect Vero cells, and the efficiency of infection was estimated by measurement of intracellular (to avoid contamination with Gluc present in the inoculum) reporter activity that exclusively results from replication of ZIKVGlucRep (but not SFV-ZIKV-CprME) in ZIKV-VREP-infected cells.

At 24 h p.i., Gluc activity was comparable with that in supernatants of Vero cells transfected with ZIKVGlucRep RNA; over the next 24 h it further increased approximately threefold (Fig. 6b). These data clearly demonstrate successful formation and release of ZIKV-VREPs in C6/36 cells as well as the entry and replication of packaged ZIKVGlucRep RNA in ZIKV-VREP-infected Vero cells. To our knowledge, this is the first example of successful ZIKV replicon packaging. Furthermore, the novel method of ZIKV VREP production developed in this study (Fig. 6c) may be used for replicon packaging of different flaviviruses.

DISCUSSION

Studies on the molecular biology of viruses, virus–host interactions and the development of vaccines or antivirals are dependent on the availability of advanced experimental tools, including efficient reverse genetics systems. Many aspects of ZIKV biology and infection are poorly understood, especially its ability to cause rare but serious neurological complications. ZIKV adapted to replication in artificial models and/or in cell culture may lack such an ability and therefore clone-derived viruses should correspond to patient–derived isolates as closely as possible. It is also important that clone-derived viruses represent South American isolates in general. Furthermore, the samples should preferably originate from the early stage of the outbreak as it avoids later adaptations that may complicate analysis of the original properties of introduced viruses.

Due to the existence of RNA viruses in the form of quasispecies, and their fast evolution and rapid adaptations to cell culture, the construction of icDNA clones with desired properties using virus propagation followed by reverse transcription, cDNA synthesis and PCR amplification is challenging. Generally, use of these approaches results in clones that differ from the consensus sequence of the respective natural isolate. More often than not, such changes arising from errors of cDNA synthesis/PCR reaction or representing naturally occurring sequence variations have a negative impact on the fitness of the virus rescued from such clones [16, 23, 24]. In contrast, synthetic cDNA clones that correspond to the consensus sequence of the natural virus isolate effectively capture the biological properties of the original virus. Furthermore, such clones can be based on sequences of patient-derived viruses with little or no history of cell culture passage.

Although the use of synthetic DNA technology allows construction of non-natural consensus clones, we chose to copy a genuine ZIKV isolate BeH819015 using available next-generation sequencing data (GI : 975885966). BeH819015 was selected because it was isolated early in the outbreak. It is also representative of the most prominent group of ZIKV isolates from South America [20] and its polyprotein sequence is very close to the consensus sequence of ZIKV isolates from South America. Furthermore, as ZIKV isolates from South America are very similar to each other, the polyprotein of BeH819015 differs from other sequenced isolates by only a few amino acid residues. For example, there are only three differences compared to PRVABC59 and six differences compared to PE243/2015. Thus, it was reasoned that the isolate would provide a good representation of all ZIKV isolates from this outbreak.

The replication of the virus rescued from the icDNA clone was identical to that of natural isolate PRVABC59 in all cell types tested. Its initial multiplication in Vero cells was clearly not optimal as during the first few passages more rapid replication and CPE induction, both indicating adaptation to cell culture, were observed. Thus, properties common for natural viruses with no cell culture passage history, were reproduced by clone-derived ZIKV. The apparent adaptation to cell culture conditions also indicated that excessive *in vitro* passaging of clone-derived virus should be avoided. For icDNA-derived viruses the low rescue efficiency (correlates with slower CPE development) indicates that successful rescue occurred in relatively few transfected cells and subsequent replication and spread of virus in cell culture was required. Conversely, fast CPE development is a consequence of rescue of the virus in a large number of transfected cells with no (or limited) subsequent spread in culture. Hence, in order to minimize cell culture adaptation (and, for marker viruses, possible loss of marker) during virus spread, the ideal system should provide high rescue efficiency. This means that, at least for constructs described in this paper, a single plasmid system is superior to a two-plasmid system and SP6 polymerase generated transcripts are superior to the plasmid with a CMV promoter. This scenario most likely applies for other systems described in the literature [16, 19, 25].

Marker-expressing viruses are useful tools for various *in vitro* and *in vivo* applications. For flaviviruses, several approaches for marker insertion have been reported, with use of an internal ribosome entry site (IRES) being the most common. We chose an IRES-free approach as ZIKV infects both vertebrate and mosquito cells and IRES elements typically work in either one or the other of these cell types, but not in both. As this approach also requires sequence duplication (Fig. 4a), we adapted our previous work with SFV mutants containing two copies of the nsP3-encoding region [24]. The use of a codon-altered copy of the capsid gene allowed production of very stable ZIKV-NanoLuc, ZIKV-EGFP and ZIKV-mCherry viruses that work well in both vertebrate and mosquito cells. In contrast, viruses containing larger insertions (FfLuc2, RSLuc) or ubiquitin in addition to EGFP and mCherry were unstable or displayed reduced stability (Fig. 4b–e). Interestingly, neither ZIKV-EGFP-Ubi nor ZIKV-mCherry-Ubi reverted back to wt virus: this would have been detected in our assay as the appearance of an RT-PCR product with a length of 486 bp, but this band was not observed (Fig. 4e). These data indicate that altering codons in the duplicated copy of the capsid encoding region prevented, or at least hugely reduced, homologous copy-choice recombination between these sequences. While it is still certain that with longer-term

passaging even the most stable marker viruses would lose marker expression (if not due to marker elimination then due to accumulation of point mutations), this phenomenon is largely irrelevant due to more rapid appearance of undesired cell culture adaptations. In fact, it is remarkable that at least for ZIKV-NanoLuc and ZIKV-EGFP (Fig. 4e) adaptation to faster growth in cell culture did not occur as a result of loss of inserted sequences.

Here we report the first ZIKV replicon using an SFV-based packaging system. At this stage, the system's efficiency remains relatively modest. This is partly due to technical difficulties: for high efficiency, large amounts of replicon RNA (difficult to obtain using a single-copy plasmid as a template for *in vitro* transcription) and efficient transfection procedures are needed. Both of these factors are more important for non-propagative replicons than for full viruses that spread in the infected cell cultures. In addition, the system will benefit from improvements such as optimization of production cell lines and of m.o.i. for infection with packaging constructs, and use of mutations attenuating cytotoxicity of SFV. However, the efficiency of replicons based on ZIKV BeH819015 will most likely remain significantly below that observed for replicons developed from cell culture-adapted flaviviruses. Hence, the moderate efficiency of our replicon system directly reflects the properties of the original patient-derived virus, which should be regarded as a strong advantage.

In conclusion, we have developed an easy-to-use reverse genetic system for ZIKV isolated from Brazil in 2015. In all *in vitro* assays the clone-derived virus was indistinguishable from a related South American ZIKV isolate. Recombinant viruses expressing small marker proteins demonstrated properties similar to wt virus and had superb genetic stability. This has allowed us to use ZIKV-NanoLuc-Ubi for the analysis of compounds inhibiting ZIKV infection [26] and makes these viruses useful tools for different *in vitro* and *in vivo* applications. We also describe the first packaging system for ZIKV subgenomic replicons. Similar to the icDNA-rescued viruses, the subgenomic replicon displays properties characteristic of patient-derived (not cell culture-adapted) viruses. In applications where high assay sensitivity is critical, the relatively low efficiency of such a replicon vector may present challenges; however, the system's high similarity to clinical isolates provides a crucial advantage for many applications.

METHODS

Cell culture

Vero E6 (hereafter Vero) cells (ATCC CCL-81) were grown in Dulbecco's modified Eagle's medium (DMEM, Gibco) supplemented with 10 % FBS (GE Healthcare). BHK-21 cells were grown in Glasgow's minimal essential medium (Gibco) containing 10 % FBS, 2 % tryptose phosphate broth, and 20 mM HEPES. BeWo cells (choriocarcinoma human placental epithelial cells; ATCC CCL-98) were maintained in Kaighn's modification of Ham's F-12 medium supplemented with 10 % FBS. hCMEC/D3 cells (human brain endothelial cells) were maintained in endothelial basal medium −2 supplemented with 5 % FBS, 1.4 µM hydrocortisone, 5 µg ml^{-1} ascorbic acid, 1 % chemically defined lipid concentrate, 10 mM HEPES, and 1 ng ml^{-1} basic fibroblast growth factor [27]. Mosquito *Aedes albopictus* C6/36 cells (ATCC CRL1660) were grown in Leibovitz's L-15 medium (Gibco) supplemented with 10 % heat-inactivated FBS (Gibco, ThermoFisher Scientific). Penicillin (100 U ml^{-1}) and streptomycin (0.1 mg ml^{-1}) were added to all growth media. Mammalian cells were cultured in a humidified incubator at 37 °C with 5 % CO_2; C6/36 cells at 28 °C without CO_2.

Source of ZIKV sequence

Sequences of four ZIKV strains isolated at the early stages of the South American outbreak and covering the complete coding region of the genome were sourced from GenBank (available as 1.02.2016). Polyprotein encoded by ZIKV isolate BeH819015 (GI : 975885966; isolated in Brazil in 2015) was the closest to the overall consensus sequence. As sequences of the 5′- and 3′- UTR ends of BeH819015 were not available, sequences of these highly conserved regions were taken from the sequence of closely related early Brazilian ZIKV isolate PE243/2015 (GI : 1026288139). For cloning purposes, a single synonymous substitution (G8411 to A) was introduced to the coding region of the viral sequence.

Design and assembly of ZIKV icDNA clones

The sequence of ZIKV cDNA was split into four fragments. Fragment A contained sequences corresponding to both flanks of ZIKV genome (residues 1–1103 and 9126–10 807) separated by recognition sites for *Sal*I, *Sma*I, *Nae*I and *BstB*I. Three versions of fragment A were designed. A-SP6 had a bacteriophage SP6 RNA polymerase promoter placed upstream of the residue corresponding to the 5′ end of the ZIKV genome, and a recognition site of restriction endonuclease *Age*I was placed immediately downstream of residue 10807, corresponding to the 3′ end of the ZIKV genome. A-SP6Rz had a similar design except that the sequence of hepatitis delta virus (HDV) antigenomic strand ribozyme was inserted downstream of residue 10 807 and was followed by the recognition site of restriction endonuclease *Pme*I. A-CMV had the immediate early promoter of human cytomegalovirus (HCMV) upstream of the residue corresponding to the 5′ end of the ZIKV genome and HDV antigenomic strand ribozyme sequence downstream of residue 10807, followed by late transcription terminator of SV40. In addition, the second intron from the human β-globin gene was inserted between residues corresponding to positions 335 and 336 of the ZIKV genome. Fragments B (residues 1098–4035), C (residues 4030–6346) and D (residues 6341–9131) were designed to contain naturally occurring recognition sequences of restriction enzymes at both of their ends (Fig. 1a). All fragments were obtained as synthetic DNAs (Genscript, USA). Fragments A-SP6, A-SP6Rz, A-CMV, C and D were cloned into a high-copy number plasmid

pUC57Kan. Fragment B was cloned into a CopyControl pCC1BAC vector (Epicentre, USA).

Plasmids containing full-length icDNA of ZIKV were assembled as follows. First, fragments A-SP6, A-SP6Rz or A-CMV were transferred into a pCC1BAC vector. Second, fragments B, C and D were added using conventional (restriction enzyme-based) cloning procedures. The constructs generated were designated as pCCI-SP6-ZIKV, pCCI-SP6-ZIKV-Rz and pCCI-CMV-ZIKV. Sequences of all plasmids were verified by Sanger sequencing and constructs were maintained and propagated as single-copy plasmids in *E. coli* Turbo strain (New England Biolabs).

Construction of ZIKV icDNAs containing sequences of reporter genes

Insertion of sequences encoding for EGFP, mCherry, NanoLuc, FfLuc2 or RSLuc into icDNA constructs of ZIKV was carried out using a similar approach to that previously described for an icDNA clone of West Nile virus [22]. Briefly, sequences of reporter genes were fused to sequences encoding for FMDV 2A autoprotease. The obtained cassette was cloned between two copies of sequence encoding for ZIKV capsid protein; from these, the codon usage of the second (downstream) copy was altered (Fig. 4a). In addition, for insertion of sequences encoding for shorter reporters (EGFP, mCherry, NanoLuc), a strategy previously described for the Dengue virus icDNA clone [21] was used, involving insertion of ubiquitin between FMDV 2A protease and the second copy of capsid protein (Fig. 4a). All eight cassettes were assembled from synthetic DNAs (Genscript, USA) and PCR fragments and cloned into the pCCI-SP6-ZIKV plasmid. The resulting constructs were designated as pCCI-SP6-ZIKV-EGFP, pCCI-SP6-ZIKV-EGFP-Ubi etc. Sequences of the plasmids were verified by Sanger sequencing.

Rescue of infectious viruses

Five micrograms of each of pCCI-SP6-ZIKV or pCCI-SP6-ZIKV-EGFP (or other construct with marker) was linearized using *Age*I restriction enzyme prior to *in vitro* transcription. For pCCI-SP6-ZIKV-Rz the linearization was carried out using *Pme*I restriction enzyme. The resulting DNA fragments were purified using NucleoSpin Gel and PCR Clean-up kit (Macherey-Nagel) and DNA Clean and Concentrator-5 (Zymo Research) columns and eluted with 6 µl water. The mMESSAGE mMACHINE SP6 transcription kit (Ambion) was used to *in vitro* transcribe RNA from 3 µl of cDNA in a 20 µl reaction volume. The capped RNA transcripts were electroporated into 8×10^6 Vero cells suspended in 800 µl of PBS [13]. In addition, 8×10^6 Vero cells were also transfected using 5 µg pCCI-CMV-ZIKV [28]. Transfected cells were monitored daily and when significant CPE was observed, the stocks of rescued viruses (p0 stocks) were harvested, centrifuged at 1000 ***g*** for 10 min to remove cellular debris and aliquots stored at −80 °C.

Virus titration and propagation

Virus titres were determined by the plaque assay as previously described [13]. Briefly, 100 µl of tenfold serial dilutions of the virus samples were added to a 12-well plate containing a confluent monolayer of Vero cells. After incubation for 1 h with shaking after every 15 min, the cells were overlaid with 1 ml of DMEM supplemented with 2 % FBS and containing 0.8 % carboxymethylcellulose (Sigma Life Science). After 4–7 days of incubation, the cells were fixed and stained with crystal violet. Visible plaques were counted and viral titres in p.f.u. ml^{-1} were calculated. To obtain p1 stocks, confluent Vero cells grown in a well of a six-well plate were infected at m.o.i. of 0.1 p.f.u. $cell^{-1}$. In some cases blind passage at low m.o.i. (using 100 µl of p0 virus stocks in 200 µl infectious media per well of a six-well plate) was used. The supernatants (p1 stocks) were collected when CPE was observed. Stocks up to p4 were obtained by repeating this procedure three more times.

Sequencing of viral stocks

Viral RNAs were extracted from 100 µl p4 stocks of viruses rescued from pCCI-SP6-ZIKV, pCCI-SP6-ZIKV-EGFP, pCCI-SP6-ZIKV-NanoLuc and pCCI-SP6-ZIKV-mCherry, as well as from lower passage stocks rescued from pCCI-SP6-ZIKV, using Quick-RNA MiniPrep kit (Zymo Research). The RNAs were reverse transcribed using the First Strand cDNA Synthesis Kit (Thermo Fisher Scientific) and PCR-amplified using ZIKV-specific primers. To identify possible second-site mutations in the p4 stock of virus rescued from pCCI-SP6-ZIKV, a set of PCR fragments covering the complete coding region of the ZIKV genome was sequenced. For the remaining viruses, only fragments corresponding to the region containing C3895 residue were sequenced.

Polyclonal antisera against ZIKV NS3 and NS5

Regions of the ZIKV genome encoding for the RNA helicase region of NS3 (aa residues 1683–2123 of ZIKV polyprotein) and RNA polymerase region of NS5 (aa residues 2772–3423 of ZIKV polyprotein) were codon optimized for *E. coli* expression. Corresponding synthetic DNAs (Genscript, USA) were cloned into the pET28(a) expression vector. Recombinant proteins were obtained using an auto-induction protocol and purified to homogeneity as previously described [29]. Soluble native recombinant NS3 and NS5 proteins were used for generation of rabbit polyclonal antibodies (Labas AS, Estonia).

Immunoblot analysis

Infected Vero cells were lysed using SDS gel loading buffer [100 mM Tris-HCl (pH 6.8), 4 % SDS, 20 % glycerol, 200 mM dithiothreitol, and 0.2 % bromophenol blue], and proteins were denatured by heating at 100 °C for 5 min. Samples corresponding to 50 000 transfected/infected cells were loaded in each well of a polyacrylamide gel. Proteins were separated by 10 % SDS-PAGE, transferred to nitrocellulose membranes, and detected using antisera against ZIKV NS3, ZIKV NS5 and EGFP (all in-house) as primary antibodies and horseradish peroxidase-conjugated goat anti-rabbit antibodies (LabAs AS) as secondary antibody.

The blots were developed and proteins visualized using ECL Immunoblot Detection kit (GE Healthcare).

ZIKV propagation and growth curve experiment

As we had no access to the original ZIKV BeH819015 isolate, we used the ZIKV PRVABC59 strain as an example of a natural ZIKV isolate. This strain was isolated in December 2015 from a patient from Puerto Rico [30] and was kindly provided by Dr David Smith (PathWest QEII Medical Centre, Western Australia). For multi-step growth curves, confluent Vero cells grown on 24-well plates were infected with the p1 stock of the icDNA clone -derived virus (icBeH819015) and PRVABC59 strain at m.o.i. 0.1 for 1 h. The inoculum was removed, cells were washed with PBS, overlaid with 0.5 ml of DMEM supplemented with 2 % FBS, and incubated in a humidified incubator at 37 °C with 5 % CO_2. At selected time points, supernatants were collected and replaced with fresh media. Virus titres were determined as described above.

Immunofluorescence microscopy

For indirect immunofluorescence microscopy, Vero cells were grown on coverslips in 24-well plates. At 50 % confluence, the cells were infected with PRVABC59, icBeH819015, ZIKV-mCherry or ZIKV-EGFP at m.o.i. of 1. At 24 h post infection (p.i.), the cells were washed with PBS, fixed with 4 % paraformaldehyde, and permeabilized with 0.02 % Triton-X-100 for 2 min. Samples were stained with rabbit anti-NS3, anti-NS5 antisera, mouse Anti-Flavivirus Group Antigen Antibody (clone D1-4G2-4-15, Millipore) and mouse monoclonal antibody against dsRNA (J2; Scicons) diluted in 5 % FBS/Dulbecco PBS. Incubation with primary antibodies was followed by three washes and incubation with secondary anti-rabbit or anti-mouse antibodies conjugated to Alexa Fluor 488, 568, or 647 (Invitrogen). Nuclei were counterstained with DAPI. EGFP and mCherry were detected using their auto-fluorescence. The samples were analysed using a Nikon A1R+confocal microscope and ImageJ software.

Analysis of luciferase reporter activity in mammalian and insect cells

Vero and C6/36 cells were grown to 90 % confluency and infected with virus at m.o.i. of 0.1. At appropriate time points, the cells were washed with PBS and lysed. Cells infected with viruses expressing the NanoLuc reporter were lysed with *Renilla* Luciferase Assay Lysis Buffer (Promega), and NanoLuc activity was analysed using *Renilla* Luciferase Assay Substrate and a Glomax SIS luminometer (Promega). Cells infected with viruses expressing FfLuc2 or RSLuc markers were lysed using Passive Lysis Buffer (Promega), and activities of FfLuc2 and RSLuc were measured using Luciferase Assay Reagent and Glomax SIS luminometer (Promega).

Determination of percentage of mCherry positive plaques for ZIKV-mCherry and ZIKV-mCherry-Ubi

p0–p4 stocks of ZIKV-mCherry and ZIKV-mCherry-Ubi were titrated and used to infect Vero cells in six-well plates at 30 p.f.u. well^{-1}. Infected cells were covered with carboxymethylcellulose overlay. After 7 days incubation the cells were analysed under a fluorescence microscope and mCherry positive plaques were counted. After this overlay was removed, the cells were fixed, stained with crystal violet and visible plaques were counted. The percentage of mCherry-positive plaques was calculated.

Viral RNA extraction and RT-PCR analysis

To analyse the genetic stability of viruses harbouring NanoLuc, EGFP and mCherry reporters, the total RNA was purified from 100 µl of p0, p2 and p4 stocks using the RNeasy minikit (Qiagen). The RNA was reverse transcribed using the First-Strand cDNA synthesis kit with a random hexamer primer (Thermo Scientific). PCRs were performed using a sense primer that matched the 5′-UTR sequence (nucleotides 47–71) and an antisense primer complementary to the sequence at the beginning of the region encoding for prM (nucleotides 509–532). Plasmids containing corresponding icDNAs were used to amplify control fragments that were 1659, 1869 or 1854 bp long for viruses/icDNAs containing NanoLuc, EGFP or mCherry sequences and 1887, 2097 and 2082 bp long for viruses/icDNAs with NanoLuc-Ubi, EGFP-Ubi or mCherry-Ubi insertions, respectively. All fragments were analysed using electrophoresis in 0.8 % TAE agarose gel. The gel was stained with ethidium bromide and visualized with UV light.

Construction of ZIKV replicon with Gluc reporter

ZIKV replicon was designed using a strategy similar to that described previously for the West Nile virus replicon [31]. The region encoding for the structural part of virus polyprotein in pCCI-SP6-ZIKV was replaced by a PCR-generated fragment containing sequences encoding for mature capsid, Gluc, FMDV 2A autoprotease and the last 30 aa residues of E protein (Fig. 6a). The construct, designated as pCCI-SP6-ZIKVGlucRep, was verified by sequencing and propagated in *E. coli* Turbo cells. Transcripts of pCCI-SP6-ZIKVGlucRep were obtained as described above and transfected into Vero or BHK-21 cell by electroporation or into C6/36 cells using Lipofectamine 2000 reagent (Invitrogen).

Construction and use of a packaging system for the ZIKV replicon

The SFV replicon containing a codon-altered (to human codon preference) ZIKV structural polyprotein encoding region (designated SFV-ZIKV-CprME; Fig. 6a) was used to provide ZIKV structural proteins *in trans*. The SFV-ZIKV-CprME replicon was packaged into SFV-VREP using an SFV two helper system [32] and BHK-21 cells. The SFV-VREP particles were concentrated by ultracentrifugation through a 20 % sucrose cushion at 125 000 ***g*** for 3 h and resuspended in TNE buffer (50 mM Tris, 100 mM NaCl, 0.5 mM EDTA). SFV-VREP titration was performed by

immunofluorescence using rabbit anti-SFV nsP3 antiserum (in-house). The particles were aliquoted and stored at −80 °C.

Funding information
This study was supported by the University of Tartu, European Regional Development Fund through the Centre of Excellence in Molecular Cell Engineering, Estonia, 2014–2020.4.01.15-013 (AM), Estonian Research Council (IUT20-27; AM) and Australian National Health and Medical Research Council to SM (APP1079086). SM is the recipient of an NHMRC Senior Research Fellowship (APP1059167).

Conflicts of interest
The authors declare that there are no conflicts of interest.

References

1. **Musso D, Gubler DJ.** Zika Virus. *Clin Microbiol Rev* 2016;29:487–524.
2. **Weaver SC, Costa F, Garcia-Blanco MA, Ko AI, Ribeiro GS *et al.*** Zika virus: history, emergence, biology, and prospects for control. *Antiviral Res* 2016;130:69–80.
3. **Cao-Lormeau VM, Roche C, Teissier A, Robin E, Berry AL *et al.*** Zika virus, French polynesia, South pacific, 2013. *Emerg Infect Dis* 2014;20:1085–1086.
4. **Duffy MR, Chen TH, Hancock WT, Powers AM, Kool JL *et al.*** Zika virus outbreak on Yap Island, Federated States of Micronesia. *N Engl J Med* 2009;360:2536–2543.
5. **Heukelbach J, Alencar CH, Kelvin AA, de Oliveira WK, Pamplona de Góes Cavalcanti L.** Zika virus outbreak in Brazil. *J Infect Dev Ctries* 2016;10:116–120.
6. **Hennessey M, Fischer M, Staples JE.** Zika Virus Spreads to New Areas - Region of the Americas, May 2015–January 2016. *MMWR Morb Mortal Wkly Rep* 2016;65:55–58.
7. **Haddow AD, Schuh AJ, Yasuda CY, Kasper MR, Heang V *et al.*** Genetic characterization of Zika virus strains: geographic expansion of the Asian lineage. *PLoS Negl Trop Dis* 2012;6:e1477.
8. **Cao-Lormeau VM, Blake A, Mons S, Lastere S, Roche C *et al.*** Guillain-Barré syndrome outbreak associated with Zika virus infection in French Polynesia: a case-control study. *Lancet* 2016;387:1531–1539.
9. **Cauchemez S, Besnard M, Bompard P, Dub T, Guillemette-Artur P *et al.*** Association between Zika virus and microcephaly in French Polynesia, 2013–15: a retrospective study. *Lancet* 2016;387:2125–2132.
10. **Schuler-Faccini L, Ribeiro EM, Feitosa IM, Horovitz DD, Cavalcanti DP *et al.*** Possible association between Zika virus infection and microcephaly - Brazil, 2015. *MMWR Morb Mortal Wkly Rep* 2016;65:59–62.
11. **Brasil P, Pereira JP Jr, Moreira ME, Ribeiro Nogueira RM, Damasceno L *et al.*** Zika virus infection in pregnant women in Rio de Janeiro. *N Engl J Med* 2016;375:2321–2334.
12. **Mlakar J, Korva M, Tul N, Popović M, Poljšak-Prijatelj M *et al.*** Zika virus associated with microcephaly. *N Engl J Med* 2016;374:951–958.
13. **Shan C, Xie X, Muruato AE, Rossi SL, Roundy CM *et al.*** An infectious cDNA clone of Zika virus to study viral virulence, mosquito transmission, and antiviral inhibitors. *Cell Host Microbe* 2016;19:891–900.
14. **Liu Y, Liu J, du S, Shan C, Nie K *et al.*** Evolutionary enhancement of Zika virus infectivity in aedes aegypti mosquitoes. *Nature* 2017;545:482–486.
15. **Schwarz MC, Sourisseau M, Espino MM, Gray ES, Chambers MT *et al.*** Rescue of the 1947 Zika virus prototype strain with a cytomegalovirus promoter-driven cDNA clone. *mSphere* 2016;1:e00246-16.
16. **Tsetsarkin KA, Kenney H, Chen R, Liu G, Manukyan H *et al.*** A full-length infectious cDNA clone of Zika virus from the 2015 epidemic in Brazil as a genetic platform for studies of virus-host interactions and vaccine development. *MBio* 2016;7:e01114-16.
17. **Deng CL, Zhang QY, Chen DD, Liu SQ, Qin CF *et al.*** Recovery of the Zika virus through an *in vitro* ligation approach. *J Gen Virol* 2017;98:1739–1743.
18. **Weger-Lucarelli J, Duggal NK, Brault AC, Geiss BJ, Ebel GD.** Rescue and characterization of recombinant virus from a new world Zika virus infectious clone. *J Vis Exp* 2017;124:e55857.
19. **Weger-Lucarelli J, Duggal NK, Bullard-Feibelman K, Veselinovic M, Romo H *et al.*** Development and characterization of recombinant virus generated from a new world Zika virus infectious clone. *J Virol* 2017;91:e01765-16.
20. **Widman DG, Young E, Yount BL, Plante KS, Gallichotte EN *et al.*** A reverse genetics platform that spans the Zika virus family tree. *MBio* 2017;8:e02014-16.
21. **Schoggins JW, Dorner M, Feulner M, Imanaka N, Murphy MY *et al.*** Dengue reporter viruses reveal viral dynamics in interferon receptor-deficient mice and sensitivity to interferon effectors in vitro. *Proc Natl Acad Sci USA* 2012;109:14610–14615.
22. **McGee CE, Shustov AV, Tsetsarkin K, Frolov IV, Mason PW *et al.*** Infection, dissemination, and transmission of a West Nile virus green fluorescent protein infectious clone by *Culex pipiens quinquefasciatus* mosquitoes. *Vector Borne Zoonotic Dis* 2010;10:267–274.
23. **Ferguson MC, Saul S, Fragkoudis R, Weisheit S, Cox J *et al.*** Ability of the encephalitic arbovirus Semliki forest virus to cross the blood-brain barrier is determined by the charge of the E2 glycoprotein. *J Virol* 2015;89:7536–7549.
24. **Saul S, Ferguson M, Cordonin C, Fragkoudis R, Ool M *et al.*** Differences in processing determinants of nonstructural polyprotein and in the sequence of nonstructural protein 3 affect neurovirulence of Semliki forest virus. *J Virol* 2015;89:11030–11045.
25. **Atieh T, Baronti C, de Lamballerie X, Nougairède A.** Simple reverse genetics systems for Asian and African Zika viruses. *Sci Rep* 2016;6:39384.
26. **Varghese FS, Rausalu K, Hakanen M, Saul S, Kümmerer BM *et al.*** Obatoclax inhibits alphavirus membrane fusion by neutralizing the acidic environment of endocytic compartments. *Antimicrob Agents Chemother* 2017;61:e02227-16.
27. **Weksler B, Romero IA, Couraud PO.** The hCMEC/D3 cell line as a model of the human blood brain barrier. *Fluids Barriers CNS* 2013;10:16.
28. **Hashemi A, Roohvand F, Ghahremani MH, Aghasadeghi MR, Vahabpour R *et al.*** Optimization of transfection methods for Huh-7 and Vero cells: comparative study. *Tsitol Genet* 2012;46:347–353.
29. **Utt A, Das PK, Varjak M, Lulla V, Lulla A *et al.*** Mutations conferring a noncytotoxic phenotype on chikungunya virus replicons compromise enzymatic properties of nonstructural protein 2. *J Virol* 2015;89:3145–3162.
30. **Shabman R, Shilts M, Puri V, Dilley K, Fedorova N *et al.*** Zika virus strain ZIKV/Homo sapiens/PRI/PRVABC59/2015. *Complete genome* 2016.
31. **Shan C, Li X, Deng C, Shang B, Xu L *et al.*** Development and characterization of West Nile virus replicon expressing secreted *Gaussia* luciferase. *Virol Sin* 2013;28:161–166.
32. **Smerdou C, Liljeström P.** Two-helper RNA system for production of recombinant Semliki forest virus particles. *J Virol* 1999;73:1092–1098.